Biochimica et Biophysica Acta 1828 (2013) 2496–2505

Contents lists available at SciVerse ScienceDirect

Biochimica et Biophysica Acta

journal homepage: www.elsevier.com/locate/bbamem

Ascorbyl palmitate interaction with phospholipid monolayers: Electrostatic and rheological preponderancy

Milagro Mottola [a], Natalia Wilke [a], Luciano Benedini [b], Rafael Gustavo Oliveira [a], Maria Laura Fanani [a,*]

[a] Centro de Investigaciones en Química Biológica de Córdoba (CIQUIBIC-CONICET), Departamento de Química Biológica, Facultad de Ciencias Químicas, Universidad Nacional del Córdoba, Haya de la Torre y Medina Allende, Ciudad Universitaria, X5000HUA Córdoba, Argentina
[b] Instituto de Química del Sur (INQUISUR-CONICET), Departamento de Química, Universidad Nacional del Sur, 8000FTN Bahía Blanca, Argentina

ARTICLE INFO

Article history:
Received 29 March 2013
Received in revised form 1 June 2013
Accepted 13 June 2013
Available online 24 June 2013

Keywords:
Gibbs monolayers
Brewster angle microscopy
Liquid-condensed domains
Vitamin C derivatives

ABSTRACT

Ascorbyl palmitate (ASC_{16}) is an anionic amphiphilic molecule of pharmacological interest due to its antioxidant properties. We found that ASC_{16} strongly interacted with model membranes. ASC_{16} penetrated phospholipid monolayers, with a cutoff near the theoretical surface pressure limit. The presence of a lipid film at the interface favored ASC_{16} insertion compared with a bare air/water surface. The adsorption and penetration time curves showed a biphasic behavior: the first rapid peak evidenced a fast adsorption of charged ASC_{16} molecules to the interface that promoted a lowering of surface pH, thus partially neutralizing and compacting the film. The second rise represented an approach to the equilibrium between the ASC_{16} molecules in the subphase and the surface monolayer, whose kinetics depended on the ionization state of the film. Based on the Langmuir dimiristoylphosphatidylcholine + ASC_{16} monolayer data, we estimated an ASC_{16} partition coefficient to dimiristoylphosphatidylcholine monolayers of 1.5×10^5 and a $\Delta G_p = -6.7$ kcal·mol^{-1}. The rheological properties of the host membrane were determinant for ASC_{16} penetration kinetics: a fluid membrane, as provided by cholesterol, disrupted the liquid-condensed ASC_{16}-enriched domains and favored ASC_{16} penetration. Subphase pH conditions affected ASC_{16} aggregation in bulk: the smaller structures at acidic pHs showed a faster equilibrium with the surface film than large lamellar ones. Our results revealed that the ASC_{16} interaction with model membranes has a highly complex regulation. The polymorphism in the ASC_{16} bulk aggregation added complexity to the equilibrium between the surface and subphase form of ASC_{16}, whose understanding may shed light on the pharmacological function of this drug.

1. Introduction

Ascorbyl palmitate (ASC_{16}) is a molecule of potential pharmacological (as well as alimentary and cosmetic) interest. It is known that ASC_{16} retains the same radical-scavenging properties of ascorbic acid and that its antioxidant efficiency is comparable to that of other natural reducing agents, such as carotenes, polyphenols, and tocopherols. Its amphiphilic nature allows these vitamin C derivatives to form aggregates that may provide an appropriate environment for the solubilization of hydrophobic and sensitive drugs [1].

ASC_{16} has a complex surface behavior, which is highly sensitive to subphase conditions. Its properties were previously studied using Langmuir monolayers and Brewster angle microscopy (BAM) [2]. Similar to the related compound ascorbyl stearate [3], ASC_{16} form stable monolayers at room temperature. But while ascorbyl stearate shows a completely condensed behavior in the whole surface pressures range, ASC_{16} monolayers show phase transition from a liquid-expanded (LE) to a liquid-condensed (LC) or crystalline phase, depending on the electrostatic properties of the film. Using a theoretical approach, we were able to explain the behavior of the ASC_{16} film at different bulk pHs and salt conditions, based on the surface pH and the dissociation fraction of the ASC_{16} molecules organized at the monolayer [2].

The ascorbic acid group in the ASC_{16} molecule contains an acidic C_3-OH group with a $pK_a = 4.2$. This indicates that in the bulk of a saline solution of pH ~ 5, the ASC_{16} monomers should exist mainly as negatively charged molecules. An important shift in the apparent pKa (~2 pH units) has been previously reported for several amphiphilic molecules when organized at an interface [4]. For stearic acid, whose pKa in bulk is ~5, it has been found an apparent pKa of 7.8–7.2 both in bilayer and monolayer systems [5,6]. The change in the environmental micropolarity of the ionizable group when organize in an interface has been reported to induce a pKa shift of only 0.2–0.4 pH units [4]. Thus, the large shift in the apparent pKa observed has been justified by the effect of a lowering of the surface pH [6]. The self-organization of an

Abbreviations: ASC_{16}, ascorbyl palmitate; DMPC, 1,2-dimyristoyl-*sn*-glycero-3-phosphocholine; DMPG, 1,2-dimyristoyl-*sn*-glycero-3-phospho-(1′-rac-glycerol); Chol, cholesterol; LE, liquid-expanded; LC, liquid-condensed; CP, collapsed phase; π, surface pressure; ΔV, surface potential; MMA, mean molecular area; Cs^{-1}, compressibility modulus; BAM, Brewster angle microscopy; DLS, dynamic light scattering; SAXS, small angle X-ray scattering

* Corresponding author. Tel.: +54 351 5353855; fax: +54 351 4334074.
E-mail address: lfanani@fcq.unc.edu.ar (M.L. Fanani).

0005-2736/$ – see front matter © 2013 Elsevier B.V. All rights reserved.
http://dx.doi.org/10.1016/j.bbamem.2013.06.016

acidic molecule into a monolayer at the air/water interface leads to a negatively charged surface and a double-layer of ions close to the interface [7]. Protons are also attracted and the surface pH becomes lower than the bulk pH, which in turn affects the ionization of the molecules at the interface. In a previous work, we demonstrated that the thermodynamic and structural properties of pure ASC_{16} monolayers depend on the surface pH and thus, on the degree of ionization of ASC_{16} molecules at the surface [2]. Over the time course of ASC_{16} monolayer compression (Langmuir film isotherms) or of the formation of Gibbs monolayers (adsorption or penetration), the charge density of the monolayer increases while the area per ionizable molecule decreases. As a consequence, the surface pH falls partially, as shown in Fig. 1a, thus neutralizing the ASC_{16} molecules at the monolayer (Fig. 1b and [2]).

The ionizable property of ASC_{16}, combined with its capacity of self-organization in surface films [2], introduces a complexity in its physicochemical behavior which is interesting in itself as a particular amphiphilic model, in addition to its pharmacological application. Therefore, we were interested in investigating the ASC_{16} interaction with model biological membranes. Early attempts in this line of study were reported by Casal's group in an investigation of ASC_{16} interaction with phospholipid bilayers [8]. These authors reported that the stabilization of the gel phase of phosphatidylcholine (PC) shifted the gel stage to a liquid-crystalline one at higher temperatures. Interestingly, this effect was stronger when ASC_{16} was in its neutral form instead of its ionized form. These findings are consistent with our previous data where neutral ASC_{16} formed crystalline 2D structures, while charged ASC_{16} self-organized into a less compact (and less stable) LC phase with rounded border-domains [2].

In the present work, we further investigated ASC_{16} interaction with lipid membranes by using lipid monolayers as the membrane model. This technique allowed us to monitor not only the thermodynamic consequences of ASC_{16} insertion into membranes, but also its kinetic properties. Thus, we explored the biophysical effect of ASC_{16} adsorption to and penetration into the lipid monolayers, and also the properties of the resultant binary (phospholipid + ASC_{16}) monolayer and of the ASC_{16} saturated subphase, taking into account electrostatic and structural features. Furthermore, some aspects of the importance of the rheological properties of the membrane model were investigated by means of the introduction of cholesterol (Chol) to the lipid system.

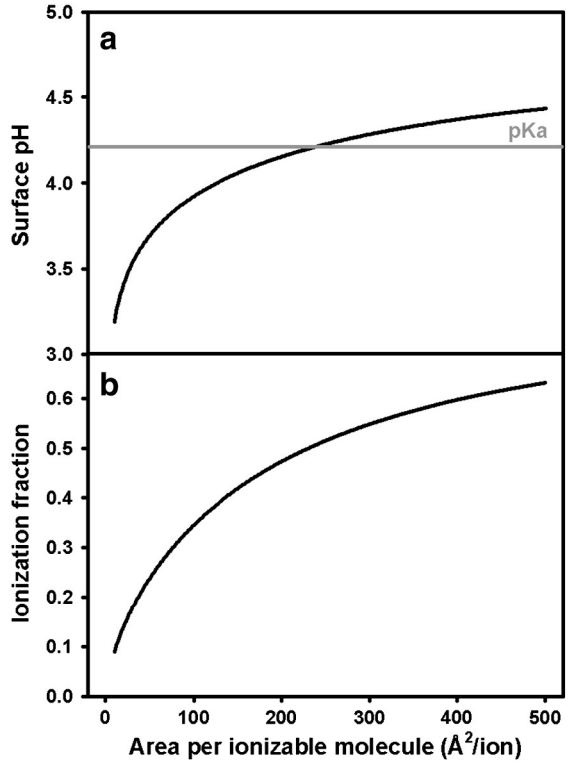

Fig 1. Ionization behavior of ASC_{16} at the interface calculated as explained in Section 2.2.6: (a) pH at the surface and (b) dissociation fraction of an acidic molecule of pKa = 4.2 as a function of the area per ion at the interface. The subphase condition was pH 5 and the subphase ion concentration was 290 mM. Horizontal gray line in (a) represents the ionization pKa of ASC_{16}. See Ref. [2].

2. Materials and methods

2.1. Materials

Ascorbyl palmitate (ASC_{16}) was purchased from Sigma-Aldrich, Co (USA). Dimiristoyl-phosphatidylcholine (DMPC), dimiristoyl-phoshatidylglycerol (DMPG) and cholesterol (Chol) were obtained from Avanti Polar Lipids, Inc (Alabama, USA). All the reagents were of analytical grade (99% pure) and used without further purification. The water was purified by a Milli-Q (Millipore, Billerica, MA) system, to yield a product with a resistivity of ~18.5 MΩ. The absence of surface-active impurities was routinely checked as described elsewhere [9].

2.2. Methods

2.2.1. Surface pressure (π)-area isotherms

Compression isotherms were obtained for DMPC/ASC_{16} and DMPC/Chol/ASC_{16} mixed Langmuir monolayers as detailed in [2]. Compression isotherms are reported as surface pressure (π) vs. mean molecular area (MMA) plots. The MMA reported is the total monolayer area divided by the total number of molecules at the interfaces. Briefly, a chloroformic solution of lipid/ASC_{16} was spread onto the surface of a Teflon™ trough filled with NaCl 145 mM as the subphase. After solvent evaporation and relaxation at $\pi \leq 0.1$ mN/m, the film was compressed isometrically at a rate of 2 ± 1 $Å^2 \cdot molec^{-1} \cdot min^{-1}$ until reaching the target pressure. π was determined with a Pt plate using the Wilhelmy method. The equipment used was a KSV Microtrough (KSV NIMA_Biolin Scientific AB, Västra Frölunda Suecia). All experiments were carried out under a N_2 stream to prevent ASC_{16} oxidation.

2.2.2. Adsorption to and penetration of ASC_{16} into the air/water surface

Adsorption experiments were performed by injections of typically 100 μL of ASC_{16} in ethanol into the aqueous subphase of a Teflon trough under continuous stirring (trough volume: 15 mL; final subphase concentration unless otherwise indicated was 18.5 μM ASC_{16}). The changes in π at constant area were registered as a function of time, while a Gibbs monolayer was established at the air/water surface. For penetration experiments, a phospholipid monolayer was formed previous to ASC_{16} injection into the subphase, by deposition of a chloroformic solution of lipids at the air/water interface, until achieving the target π. The phospholipid monolayers were (initially) pure DMPC or DMPC/cholesterol at 30 mN/m (unless otherwise indicated). We chose NaCl solution as aqueous solvent for studying ASC_{16} behavior to keep the system as simple as possible. The aqueous solutions used as the subphase were: saline solution pH 5 (NaCl 145 mM, whose final pH after ASC_{16} addition is $pH = 5.0 \pm 0.2$), saline solution pH 3 (NaCl 145 mM adjusted to pH 3 with HCl, whose final pH after ASC_{16} addition is $pH = 2.8 \pm 0.2$) or saline solution pH 8 (NaCl 100 mM buffered with TrisHCl 10 mM at pH 8), as indicated. In the latter condition the buffer was added in order to avoid acidification due to dissolution of atmospheric CO_2. The equipment used was a homemade circular Langmuir balance controlled by an electronic unit (Monofilmetter, Mayer, Gottingen). Equilibrium values of π and $t_{1/2}$ were calculated by fitting the second part of each curve with a hyperbolic function of the type: $\pi = \pi_{eq} t / (t_{1/2} + t)$. All experiments were performed at 24 ± 2 °C. All experiments were carried out under a N_2 stream to prevent ASC_{16} oxidation.

2.2.3. Surface potential measurements

Simultaneous to compression isotherms or adsorption/penetration experiments, the Volta surface potential (ΔV) was monitored using an air-ionizing ^{241}Am surface electrode placed ~5 mm above the interface and an Ag/AgCl/Cl$^-$(3 M) reference electrode dipped into the subphase [10]. ΔV = 0 was defined at the bare air/water interface voltage prior to each experiment.

2.2.4. Compressibility analysis of Langmuir and Gibbs films

In order to analyze the elastic behavior of the films, the compressibility modulus (Cs^{-1}) was calculated as follows [7]:

$$C_s^{-1} = -A\left(\frac{d\pi}{dA}\right)_T \quad (1)$$

where *A* represents the total monolayer area. For Langmuir isotherms, the *dπ/dA* data was obtained from regular compression experiments. For penetration experiments, the monolayer was compressed at a rate of 3 $Å^2 \cdot molec^{-1} \cdot min^{-1}$ after the ASC_{16} penetration experiment reached a stable π value (30–50 min) and the slope of the π vs. *A* plot was then used to calculate the Cs^{-1}.

2.2.5. BAM visualization

Langmuir monolayers were prepared as described above using a KSV Microtrough apparatus (KSV NIMA-Biolin Scientific AB, Västra Frölunda Suecia). The Langmuir equipment was mounted on the stage of a Nanofilm EP3 Imaging Ellipsometer (Accurion, Goettingen, Germany), which was used in the Brewster Angle Microscopy (BAM) mode. Minimum reflection was set with a polarized 532 λ laser incident on the bare aqueous surfaces at the experimentally calibrated Brewster angle (~53.1°). After monolayer formation, and during compression, the reflected light was collected with a 20× objective. The gray level at each pixel of the BAM images can be converted to reflectivity values after calibration factors are set for each individual experiment. The reflectivity obtained from BAM measurements is directly related to the square of the film thickness and to the refraction index of the film [11]. For a better visualization, in Figs. 4, S1 and S2, the lower 0–70 gray level range (from the 0–255 original scale) was selected in order to maintain the gray level to film thickness relationship. This experimental setup does not allow keeping a N_2 enriched environment, therefore to prevent ASC_{16} oxidation the experiments were performed in less than 30 min. Control experiment showed that the compression isotherm of ASC_{16} does not significantly change when the film was exposed to the air during this lapse of time.

2.2.6. Ionization state of ASC_{16} as a function of the bulk pH

As described in detail in [2,6], a monolayer of charged molecules leads to a double-layer of ions, thus attracting protons to the surface and inducing a lowering of the surface pH (pH_s) as follows [7]:

$$pH_s = pH_b + F\psi_0/2.3RT \quad (2)$$

where *F* is the Faraday constant and *RT* is the thermal energy. Since ψ_0 is a function of the surface charge density [6] and pH_s, and therefore the degree of dissociation (α) of the ASC_{16} molecules in turn depends on ψ_0 [4], with a mutual regulation being established and introducing further complexity. Since there is no analytical solution, a numerical approach was used as described in [6] to obtain the pH_s, ψ_0 and α for a given subphase and surface packing (area per ionizable molecule) condition.

2.2.7. Dynamic light scattering (DLS)

In order to analyze the structure of ASC_{16} in aqueous solution, we employed DLS to evaluate the frequency of sizes and population distribution of the aggregates. The samples were prepared by dilution of a concentrated stock of ASC_{16} in ethanol in saline solutions of pH 5, pH 3 and pH 8 at a, final ethanol concentration of 0.6% (see Section 2.2.2). Accumulative data were collected by 15 min analysis of 0.4 mL of 18.5 μM ASC_{16} solutions. The equipment used was a Submicron Particle Sizer NICOMP 380 (PSS-NICOMP Santa Barbara, California, USA).

2.2.8. Nephelometry

The light reflected by 1 mL of ASC_{16} suspension at the μM range was collected by a photoreceptor at 90° from the incident beam (λ 530 nm) in a Fluorescence Spectrophotometer (Cary Eclipse, Varian Medical Systems, Inc. Palo Alto, CA). The samples were prepared as described in Section 2.2.7. Since typical CMC studies (partition of probes such as ANS and Sudan Black) failed in detecting ASC_{16} aggregates probably because of a tighter structure compared to typical lipid or detergent micelles, we used nephelometry signal to assess the monomer concentration in equilibrium with the bulk aggregates. The equilibrium monomer concentration (EMC) was then estimated by extrapolation to zero reflection of the nephelometry signal vs. ASC_{16} concentration plots.

2.2.9. SAXS measurements

SAXS was performed using the SAXS2 beamline at the Brazilian Synchrotron Light Laboratory (LNLS) at Campinas, Brazil. The ASC_{16} was resuspended in saline solution at pH 3, 6 and 8 (see Section 2.2.2.) at 5 mg/mL in the presence of 5% ethanol. Measurement conditions were: 5 min of exposure, 1 m sample-detector distance, 1.5 Å irradiation, and 30 °C. The buffers were measured and discounted from the signals. Data was collected by an MARCCD and radially integrated by using FIT2D V 12.077 (Andy Hammersley, ESRF). Spacings were obtained as normal for lamellar systems ($d = 2\pi/q$). The correlation length was calculated with the Scherrer equation from the full width at half the maximum values (FWHM) of the diffraction peaks $D = 0.9 \times 2\pi/FWHM$.

3. Results and discussion

3.1. Adsorption to and penetration of ASC_{16} into phospholipid interfaces

When a concentrated solution of ASC_{16} was dissolved in the bulk of an aqueous solution, the adsorption of these amphiphilic molecules to the air/water interface resulted in a Gibbs monolayer, evidenced by a decrease in the surface tension (increase of surface pressure, π, of up to ~35 mN/m) and changes in surface potential (ΔV) (Fig. 2a). In contrast with Langmuir monolayers, Gibbs monolayers reflect the equilibrium between the bulk form of the amphiphile and the organized film at the interface [7]. When ASC_{16} was added to the subphase of a pre-formed phospholipid monolayer (used as lipid model membrane) at a relatively high surface density (~30 mN/m), the π vs. time curve revealed an increase of up to values close to 55 mN/m, which was ~20 mN/m above the increase that resulted from adsorption to bare surfaces (Fig. 2b). In other words, ASC_{16} alone lowered the surface tension of the air/water interface from ~72 to ~37 mN/m, and to ~18 mN/m when incorporated in a phospholipid monolayer. These findings highlight that ASC_{16} is a potent co-amphiphile.

For a regular amphiphile, the adsorption kinetic curve can be described by a hyperbolic function [12]. However, when we recorded π vs. time for ASC_{16} experiments, a biphasic behavior appeared reproducibly with a transitory peak followed by a slow rise to equilibrium values. These two kinetic phases, which occurred in both adsorption and penetration experiments, could also be observed in simultaneously measured ΔV-time curves (Fig. 2a and b). Lowering the ASC_{16} subphase concentration resulted in a decrease of the first peak and a final rise to the equilibrium π, which was essentially constant for all subphase concentrations assayed (Fig. 2c). This result indicated that the first peak may involve out-of-equilibrium concentration dependent processes, while the second maximum represented a true equilibrium state in saturated conditions.

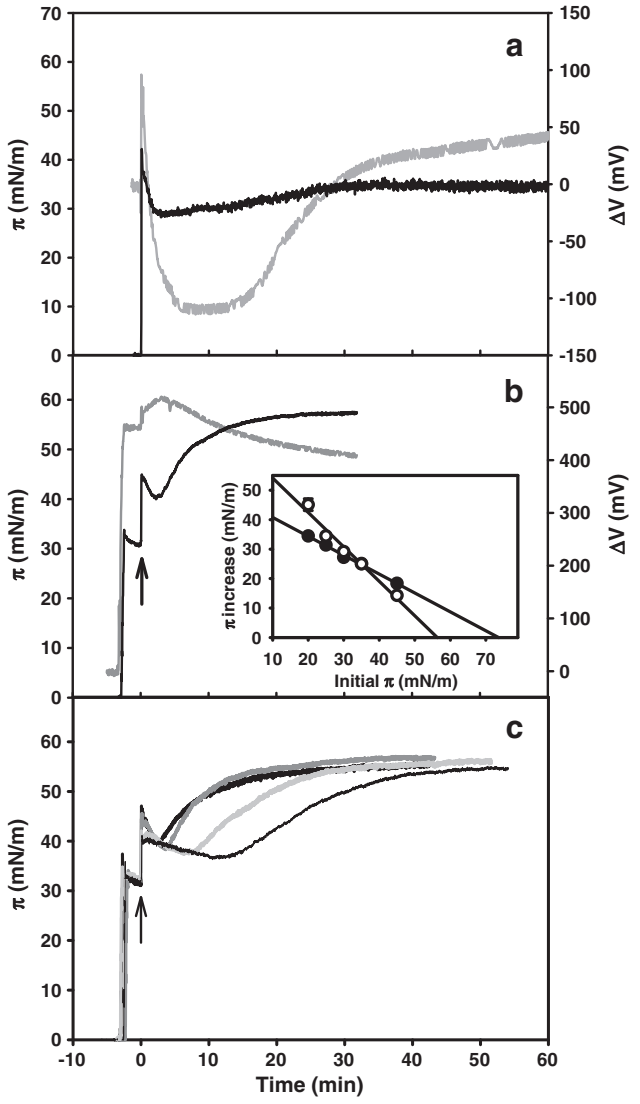

Fig. 2. Gibbs adsorbed monolayers and penetration of ASC_{16} into phospholipid monolayers: a) Gibbs monolayer of ASC_{16} formed by adsorption to a bare air/saline solution surface and (b) penetration of ASC_{16} into DMPC monolayer at ~30 mN/m. The black and gray lines in (a) and (b) correspond to the surface pressure (π) and surface potential (ΔV) time curves respectively. Final subphase conditions: ASC_{16} 18.5 μM and pH 5. c) Subphase concentration dependence of ASC_{16} penetration on DMPC monolayers at ~30 mN/m. Final subphase concentration was 18.5 μM (thick black line), 6.7 μM (dark gray line), 2.7 μM (light gray line) and 1.3 μM (thin black line). The arrows indicate the time of the ASC_{16} injection into the subphase. The curves shown are chosen from a set of duplicates that differed by less than 3 mN/m. The inset in (b) shows cutoff curve for ASC_{16} penetration into DMPC (black circles) or DMPG (open circles) monolayers at different initial π values. The results represent the average of two independent experiments ± SEM. Error bars are within the size of the point.

As discussed in the Introduction section and in [2], the acidic properties of ASC_{16} lead to a negative charged surface when it forms a monolayer at the air/water interface, and a double-layer of counterions is then attracted to the surface. In this way, the surface pH becomes lower than the bulk pH, thus affecting the ionization of ASC_{16}. Immediately after ASC_{16} injection into the saline solution, ASC_{16} self-assembled at the bare surface, which resulted in a fast overpressure phase and a peak in ΔV (Fig. 2a). As a result, the ΔV curve revealed a reorganization period (from times 5–20 min, in Fig. 2a), with negative values of ΔV being observed. This fall in ΔV values may imply the establishment of a negatively charged surface after ASC_{16} fast insertion, a phenomenon previously observed for stearic acid monolayers in its acidic form [6]. It is worth to bear in mind that the ΔV parameter is the resultant of several components, including the dipole moment normal to the interface of the amphiphiles, the surface charge density and the contribution of the hydration shield and counterions affected by the double layer potential [7,12]. Therefore, a change in this parameter should be interpreted by taking into account this complexity. When the molecular and charge densities in the monolayer increased, the surface pH fell, thereby partially neutralizing the ASC_{16} molecules at the monolayer (Fig. 1) [2]. This phenomenon may explain the fast drop after the initial pressure peak, considering previous studies showing that the neutral ASC_{16} favors the establishment of a condensed phase in comparison with the ionized ASC_{16} [2]. As a result, a phase change from the LE to LC phase would be expected upon neutralization, with a concomitant reduction in π (at constant area, which is the case for our experiments). Supporting the neutralization hypothesis, we observed an increase and stabilization of ΔV at positive values over long times.

When the ASC_{16} molecules penetrated into a previously formed DMPC monolayer, a lowering of the ΔV was observed but without a posterior rise (compare gray curves in Fig. 2a and b). This can be explained since the charge density of the ASC_{16}–DMPC monolayer might have been lower than that of pure ASC_{16} monolayers, mainly because of the lower mole fraction of the charged molecules. Therefore, the partial neutralization of the interface was less evident.

To investigate further ASC_{16} penetration into phospholipid monolayers, penetration experiments of ASC_{16} into DMPC monolayers were performed at different initial values of π. The increase in π observed after the first peak depended on the initial π, as shown in the inset of Fig. 2b. The extrapolated maximum π that ASC_{16} would be able to penetrate (cutoff point) was extremely high and close to the theoretical limit ($\pi = 72.8$ mN/m, corresponding to a null surface tension). We further explored ASC_{16} penetration into a charged monolayer of pure DMPG, and the inset in Fig. 2b shows that there was a lower π increase for DMPG monolayers at high initial π values, resulting in a cutoff point of 56 mN/m. This may be explained as repulsion between the charged monomer and the negative surface. High cutoff points were also reported previously for the cationic drug Promethazine when interacting with anionic phospholipid monolayers [13]. Interestingly, in our case, a high cutoff value was found for negatively charged amphiphiles interacting with negatively charged surfaces. This result highlights a notable potential of ASC_{16} to interact with biological membranes.

3.2. ASC_{16}/DMPC binary Langmuir films

Since the above penetration experiments involved a continuous enrichment over time (of the initially pure DMPC monolayer) with ASC_{16}, we further studied the binary ASC_{16}–DMPC monolayer system. Langmuir monolayers were used and the increase in π was registered upon compression of the film. Previous studies have tested the capacity of surface mixing of the related compound ascorbyl stearate against vitamin K [14], vitamin D_3 [15] and α-tocopherol [3]. Those mixtures show good miscibility, which is notable considering the condensed nature of ascorbyl stearate monolayers. However, as far as we know no such study has been carried on in mixtures with phospholipids.

In agreement with bibliography data, the DMPC monolayer showed characteristics of an LE phase [16] while pure ASC_{16} revealed a transition from LE to a stable LC phase at ~14 mN/m [2] (Fig. 3a). When as little as 10 mol% of ASC_{16} was added to the DMPC monolayer a LE–LC transition was observed at high π, close to the collapse pressure (CP). This transition was evidenced in the compression curve as a drop in the slope of the curve at ~38 mN/m (see arrows in Fig. 3a). As more ASC_{16} was incorporated into the film the beginning of the phase transition occurred at lower π values and the CP increased, demonstrating a stabilization of the LC phase by ASC_{16} (see inset in Fig. 3a). These smooth changes in the CP and the transition pressure with the composition revealed a good degree of mixing of the components close to

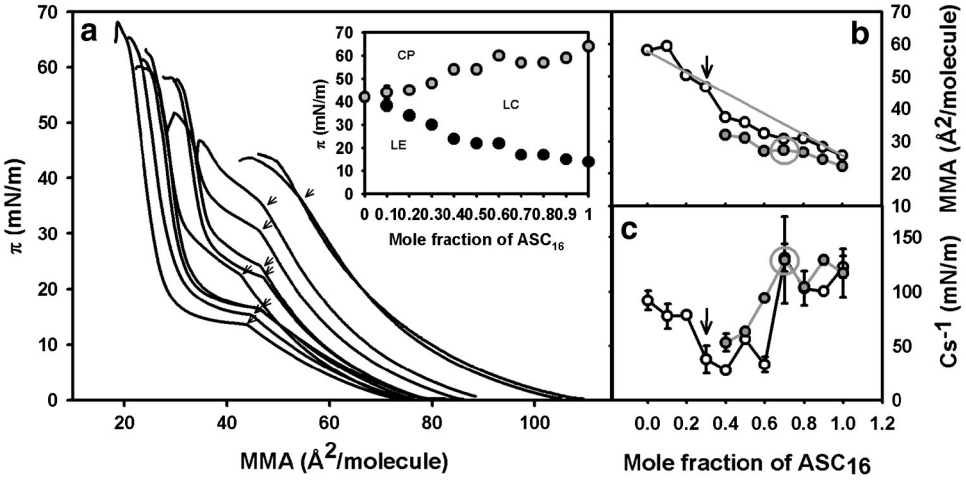

Fig. 3. Langmuir Isotherms of mixed ASC_{16} + DMPC monolayers. a) Surface pressure (π) vs. mean molecular area (MMA) curves of pure ASC_{16} or pure DMPC monolayers and mixed binary monolayers at different proportions: from left to right 1, 0.9, 0.8, 0.7, 0.6, 0.5, 0.4, 0.3, 0.2 and 0.1 mole fractions of ASC_{16} and pure DMPC. The curves shown are chosen from a set of duplicates that differed by less than 2 $Å^2$/molecule. The inset shows the phase diagram of the binary system: LE liquid-expanded phase; LC liquid-condensed phase; and CP collapsed phase. b–c) Isobaric analysis of Langmuir monolayer data: (b) MMA and (c) compressibility modulus, Cs^{-1} is shown as a function of ASC_{16} content along the 30 (white circles) or 55 mN/m (gray circles) isobars. Gray line in (b) represents the MMA of an ideal mixture after Raoult's law. Big circles highlight the area and compressibility values that correspond to typical penetration experiments. The onsets of the LE to LC transition are indicated by small arrows on the isotherms and isobars and black points in the inset in (a). The gray points in (a) correspond to the monolayers to CP transition. The results are the average of two independent experiments ± SEM. Error bars in the inset are within the size of the point.

ideality [7]. Some similarities can be found between this phase diagram and the previously reported for the binary system stearic acid + DMPC [6]. Free fatty acid represents the simplest ionizable lipids in nature and shares, beside its acidic nature, some other characteristics with the system studied in the present work: similar to stearic acid [17], ASC_{16} shows a condensed behavior in a wide range of π when it is in its neutral form and a LE → LC phase transition when charged at the interface [2]. More recently, Vega Mercado et al. [6] demonstrated a good miscibility of DMPC with stearic acid in its ionized, expanded form.

A few mN/m above the transition pressure (data obtained from isotherms), LC domains were found by BAM in the transition region. Those domains appeared as small bright spots at low ASC_{16} content, which became larger and flower-like shaped with an increase in ASC_{16}. Further compression of the binary film induced instability of the domain border (evidenced as fingered borders, see Fig. 4d–i left panel) and the merging of the phases into a single one. Only the pure ASC_{16} film showed a complete transition (not merging) from the LE to LC phase over the transition pressure range. It was notable that in the ASC_{16}-enriched samples the domains had a peculiar shape (as three lobules and a curved tail), which grew preferentially to the left side of the tail and then formed branched domains with a central hole (see Fig. 4I and j and Fig. S1). A similar phenomenon was previously observed in pure ASC_{16} monolayers [2].

The binary (DMPC + ASC_{16}) condensed phase, observed as LC domains by BAM, accounted for a stabilization of the film at a high surface pressure. This effect may have been related to that of a previous report, where the formation of hydrogen bonds between the OH group at position 3 in ASC_{16} and the ester carbonyl group at the sn-2 chain in PC was observed by infrared spectroscopy [8].

From the compression isotherms shown in Fig. 3a, valuable information can be extracted to help cast light on the penetration phenomena. In this regard, the mean molecular area (MMA) at a fixed pressure was obtained at different ASC_{16} proportions in the mixed films (see isobars in Fig. 3b). In mixed films the MMA represents the sum of the area of each component weighed by its corresponding proportion plus the deviation from ideality that results from the component interaction. The MMA was large in ASC_{16}— poor samples and smaller at ASC_{16}-rich samples, because of two combined effects: i) ASC_{16} molecules are smaller (containing only one acyl chain) than the two-tailed DMPC and ii) a general condensation of the film. As an example, at 30 mN/m pure DMPC was in the LE phase, while an incorporation of 30 mol% of ASC_{16} induced an LE–LC transition. However at 70 mol% of ASC_{16} and above the monolayers were completely in the LC state (see Fig. 3a and b).

It is important to note that the mixed monolayers became stable at 55 mN/m only after an enrichment of 40 mol% in ASC_{16}. This indicated that the penetrated monolayers, which reached ~55 mN/m, must have suffered an enrichment in ASC_{16} as high as ≥40 mol%. Additional information was extracted by means of calculation of the compressibility modulus (Cs^{-1}) of the Langmuir films (see Section 2.2.3). This parameter reflects some rheological properties of the film: LE phases respond little upon compression and gives Cs^{-1} values roughly ≤100 mN/m, while LC films respond sharply upon compression and reach higher Cs^{-1} values [7]. Fig. 3c shows the Cs^{-1} values along two isobars as a function of monolayer composition. By progressing from left to right along the 30 mN/m isobar, it can be observed that the Cs^{-1} values of 80–100 mN/m fell to lower values during the phase transition compositional range but increased to >100 mN/m at high ASC_{16} content. Other isobars showed similar behaviors (not shown) being shifted to the right for lower π and to the left to higher π.

The Cs^{-1} value for ASC_{16} penetrated monolayers at long times (initial π 30 mN/m, saline subphase pH 5) was the $Cs^{-1} = 170 \pm 20$ mN/m. A comparison of this data with information in Fig. 3b and c reveals that the penetration experiments resulted in monolayers containing 70 mol% ASC_{16} or above, and a MMA of ~27 $Å^2$/molecule. Therefore, considering a film thickness of ~1.5 nm [11] a ASC_{16} surface concentration of 2.8 M, a partition coefficient K_p of 1.5×10^5 and a $\Delta G_p = -6.7$ kcal·mol^{-1} were estimated. This K_p value is one order of magnitude greater than the partition of some amphitropic enzymes, such as sphingomyelinase to substrate monolayers [18], and of the most potent phenothiazine amphiphilic drugs [13].

3.3. The kinetic and equilibrium features of ASC_{16} penetration are affected by the electrostatic properties of the film

As discussed in the Introduction section, the self-organization of ASC_{16} at the interface induces the establishment of a charged surface, and as a consequence, a double layer of counterions. This double layer

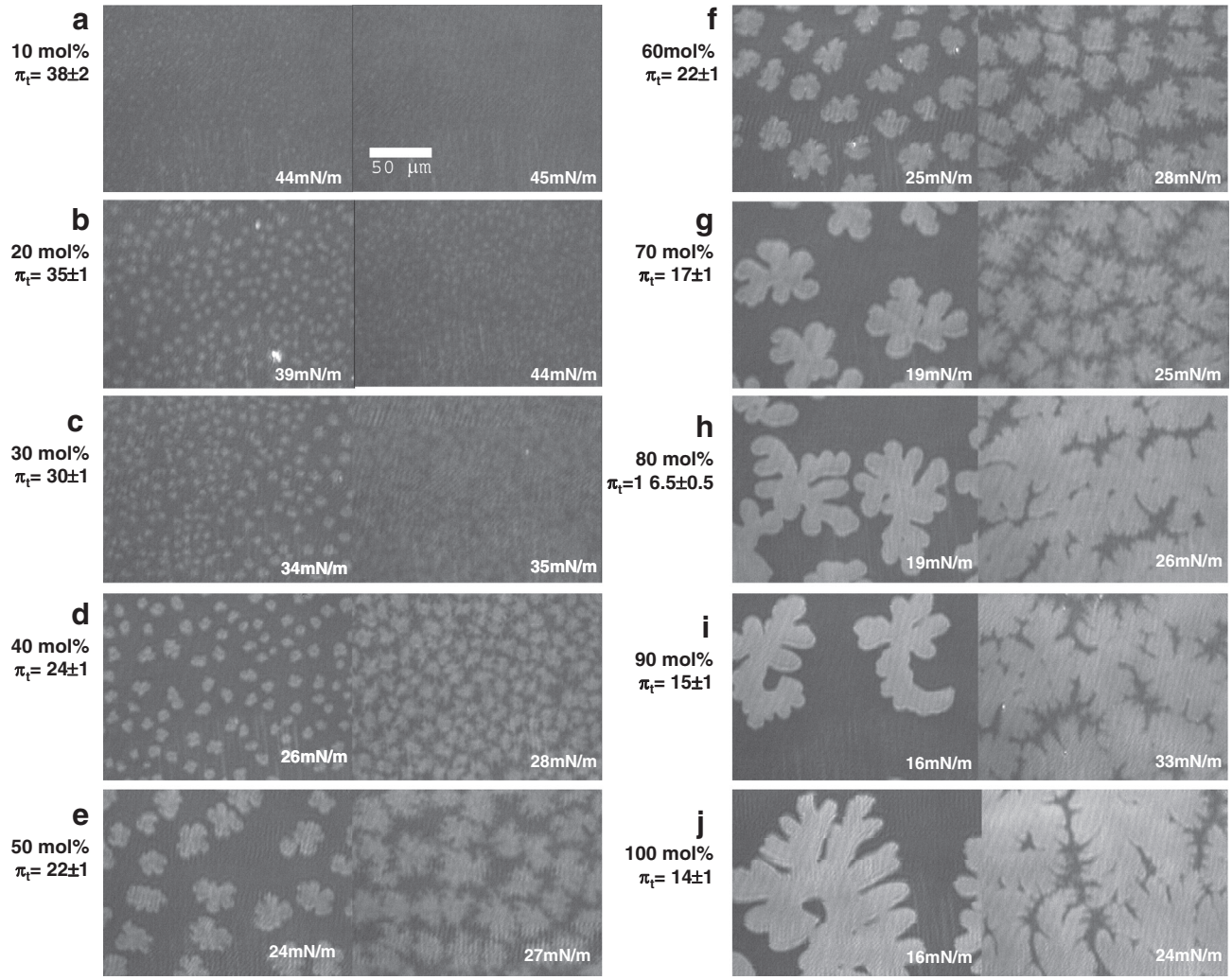

Fig. 4. BAM of binary Langmuir monolayers. The pattern of ASC_{16}–DMPC monolayers (panels a–i) or pure ASC_{16} (panel j) is shown at (left) the onset of the LE–LC phase transition (2–4 mN/m above the corresponding transition pressure, π_t) and (right) at a selected point at a higher π as indicated. The pictures are representative of two independent experiments.

is dependent on the ionic strength of the subphase and the charge density of the surface [2,7]. As shown in Fig. 1, an enrichment of the phospholipid monolayer in ASC_{16} induced a lowering of the surface pH beneath the pKa of ASC_{16} (owing to attraction of protons), thus neutralizing the surface. The surface pH calculation was based on the assumption that the pKa value (measured in bulk) does not change on the interfacial lipid environment. Thus, a pKa of 4.2 was used. If there were a pKa shift in our system due by a change in the micropolarity of the interface, it will be negligible in comparison with a much larger change in the interfacial pH [4], and will not be considered in our approach. In the previous section, we estimated that, at equilibrium and in control conditions (145 mM NaCl, pH ~ 5, room temperature), the MMA of the penetrated film was ~27 $Å^2$/molecule, with the film composition of ASC_{16} being ~70 mol%. Therefore, the effective area per ionizable molecule (ASC_{16}) would be expected to be ~39 $Å^2$. From this data and Fig. 1b, we could conclude that only a fraction of 0.21 of the total ASC_{16} molecules at the interface were charged. To validate this model, penetration experiments were performed at different subphase salt conditions (Fig. 5).

When penetration occurred at low ionic strengths (1×10^{-3} to 50 mM NaCl), the effect of the surface charge density on the subphase proton concentration was important enough to lower the ionization fraction of the film to ≤0.15 (assuming the same average molecular area and fraction of ASC_{16} was adsorbed as for 0.15 mM NaCl). Under these conditions, equilibrium was attained quickly ($t_{1/2}$ under 1 min) and reached a high equilibrium π (see inset in Fig. 5). As the ionic strength of the subphase increased, the double layer of ions was mainly composed of Na^+ and screened the charge at the surface. Therefore, the effect on the pH at the surface was weakened and the ionization fraction increased to 0.29 at 500 mM NaCl. This charged surface induced a repulsion to the charged monomers at the subphase, a phenomenon evidenced by a slowing down of the penetration process ($t_{1/2}$ ~8 min, see inset of Fig. 5).

Earlier studies demonstrated that ASC_{16}/water systems do not form micelles but produce a coagel phase, (in agreement with a critical parameter close to 1) that melts to a gel phase at ~60 °C at a water fraction of 0.5 w/v [19]. A more complete study of the lyotropic behavior of ASC_{16} has been reported [1], but still focused on highly concentrated solutions (the lower ASC_{16} concentration investigated was 0.05%). In the present work, a much more diluted amphiphile suspension was used in order to investigate ASC_{16} interaction with model membranes. Since the equilibrium between the bulk and the surface aggregates is likely to occur through its monomeric form, we further explored the equilibrium monomer concentration (EMC) at different salt conditions by nephelometry studies. We found small variation in the EMC as a function of the ionic strength of the solution ranging

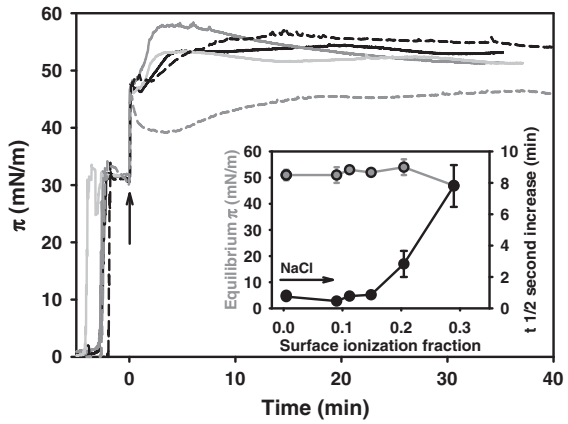

Fig. 5. Ionic strength dependence of ASC_{16} penetration into DMPC monolayers. π-time curves corresponding to the penetration of ASC_{16} into DMPC monolayers at different subphase salt conditions at pH ~ 5: pure water (black, full line), 5 mN NaCl (dark gray, full line), 50 mM NaCl (light gray, full line), 145 mM NaCl (black, dashed line) and 500 mM NaCl (gray, dashed line). The arrow indicates the time of ASC_{16} injection into the subphase. The curves shown are chosen from a set of duplicates that differed by less than 3 mN/m. The equilibrium π (gray points) and the $t_{1/2}$ of the increase to equilibrium (black points) are plotted in the inset as a function of the ionization fraction of the film at an ionic area per ionizable molecule of 39 $Å^2$/molecule. The results are the average of two independent experiments ± SEM.

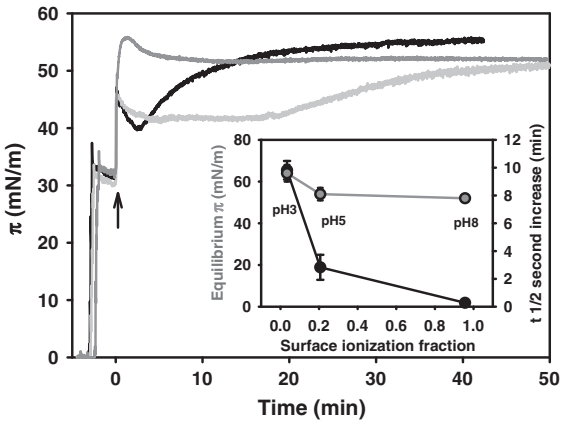

Fig. 6. pH dependence of ASC_{16} penetration into DMPC monolayer. π-time curves corresponding to the penetration of ASC_{16} into DMPC monolayers at 145 mM NaCl and the following subphase pH conditions: pH ~ 5 (black line), pH ~ 3 (light gray line) and pH ~ 8 (dark gray line). The arrow indicates the time of the ASC_{16} injection into the subphase. The curves shown were chosen from a set of duplicates that differed by less than 3 mN/m. The equilibrium π (gray points) and the $t_{1/2}$ of the rise to equilibrium (black points) were plotted in the inset as a function of the ionization fraction of the film at an area per ionizable molecule of 39 $Å^2$/molecule. The results are the average of two independent experiments ± SEM.

from 3 to 6 μM (6 ± 2, 4 ± 2 and 3 ± 1 μM for 0, 50 and 500 mM NaCl solutions). This small decrease of EMC in highly salted solution does not explain the ten folds increase in the half time of the penetration kinetics shown in Fig. 5, thus supporting the monomer-surface repulsion hypothesis.

3.4. Subphase pH affects both the ASC_{16} structure at the subphase and the penetration process

By the same reasoning as above, a change in the subphase pH will affect the surface ionization fraction of the DMPC/ASC_{16} film and, thus the penetration process. However, penetration experiments at different subphase pH values gave unexpected results: at pH ~ 8 and when the ionization fraction of the film was high (~0.95), a fast penetration was observed. In addition, at pH ~ 3, when the surface was nearly neutral, the penetration process was slow (Fig. 6). These results cannot be explained solely by means of electrostatic interactions. Therefore, the effect of the subphase pH on the structure of the subphase ASC_{16}, was now investigated.

Comparative nephelometry measurements of ASC_{16} suspensions in the micromolar range at different pHs revealed a higher reflection capacity for acidic and neutral solutions than alkaline samples (Fig. 7a). An extrapolation of the nephelometry values to zero in Fig. 7a indicates the EMC of the ASC_{16} suspensions. Our results show only a 1.7 folds increase in the EMC at pH 8 compared with the values found at neutral and acidic pH (14 ± 1, 8 ± 2 and 8 ± 1 μM for pH 3, 5 and 8, respectively). This is consistent with bibliographical data, which reports a higher solubility for the salt form of ASC_{16} than for the neutral form [20].

Dynamic light scattering (DLS) studies of these samples showed a predominant occurrence of large structures (≥700 nm diameter) at pH 3 and pH 5 (Fig. 7 b and c) that became smaller in size at pH 8 (Fig. 7d). It is important to note that at low pHs, the ASC_{16} molecules were mainly present in the neutral form, and a gel-type of aggregation may be favored in agreement with previous reports [2,19]. Even at pH 5, which is above the pKa, self-organized ASC_{16} molecules in a surface (lamellar structure?) would be able to induce the lowering of the surface pH in the same way that occurred for films formed in the air/water interface. In contrast, at high pH the charged form must dominate and the anionic amphiphile may prefer to aggregate into smaller structures.

To shed more light on the structures that existed in these samples, we determined the structural parameters by small angle X-ray scattering (SAXS). The strong diffraction peak at 1.38 nm^{-1}, plus the weaker one at 2.76 nm^{-1} (in clear relation 1:2) observed in Fig. 8, suggested that the molecules were ordered in a lamellar (smectic) phase in acidic conditions, with the resulting spacing being 4.55 nm. The presence of strong diffraction peaks (structure factor) at pH 3 and 5 showed that the membranes were strongly correlated (correlated fraction near 100%) with a high coherence length of at least 100 nm. In contrast, at pH 8, the main features were a diffuse scattering bump (the form factor, coming from the internal interference of uncorrelated or decoupled bilayers), coexisting with the previous diffraction peak, at the same location due to correlated bilayers. This revealed that in fact there were two populations of bilayers: one similar to the previous one, with the same spacing of ~4.55 nm, plus a new population of uncorrelated bilayers, with the correlated fraction dropping to ~30%. Alkaline media clearly shifted the equilibrium to membrane decoupling, probably due to increased ionization and electrostatic repulsion.

The results shown in Figs. 7 and 8 were consistent with a lamellar structure of ASC_{16} at pH 3 and 5, with the amphiphile being mainly neutral and with a shift to less structured aggregates at pH 8 when the ASC_{16} was charged. Some discrepancies can be observed on comparing the DLS and SAXS data of the pH 8 sample: DLS showed only the presence of small structures, while SAXS showed a combination of some correlated bilayers with uncorrelated structures. This may have been a consequence of the higher concentrations necessary to carry out the SAXS measurements compared with the micromolar scale of the DLS and the nephelometry experiments. Bearing in mind the above data, we can re-examine the results shown in Fig. 8. Penetration experiments at pH 8 showed a rapid kinetic when small anionic aggregates and monomeric forms of ASC_{16} are in equilibrium with phospholipid monolayers, even when the surface also became negatively charged. In contrast, neutral ASC_{16} assembled in big lamellar structures interacted slowly with neutral phospholipid monolayers. Since only a 1.7 increase was found in the EMC in alkaline conditions, the 35 folds fall in the half time of monolayer penetration in this condition (inset in Fig. 6) might be the result of a highly dynamic exchange between ASC_{16} molecules in those small charged bulk aggregated and the monomeric form.

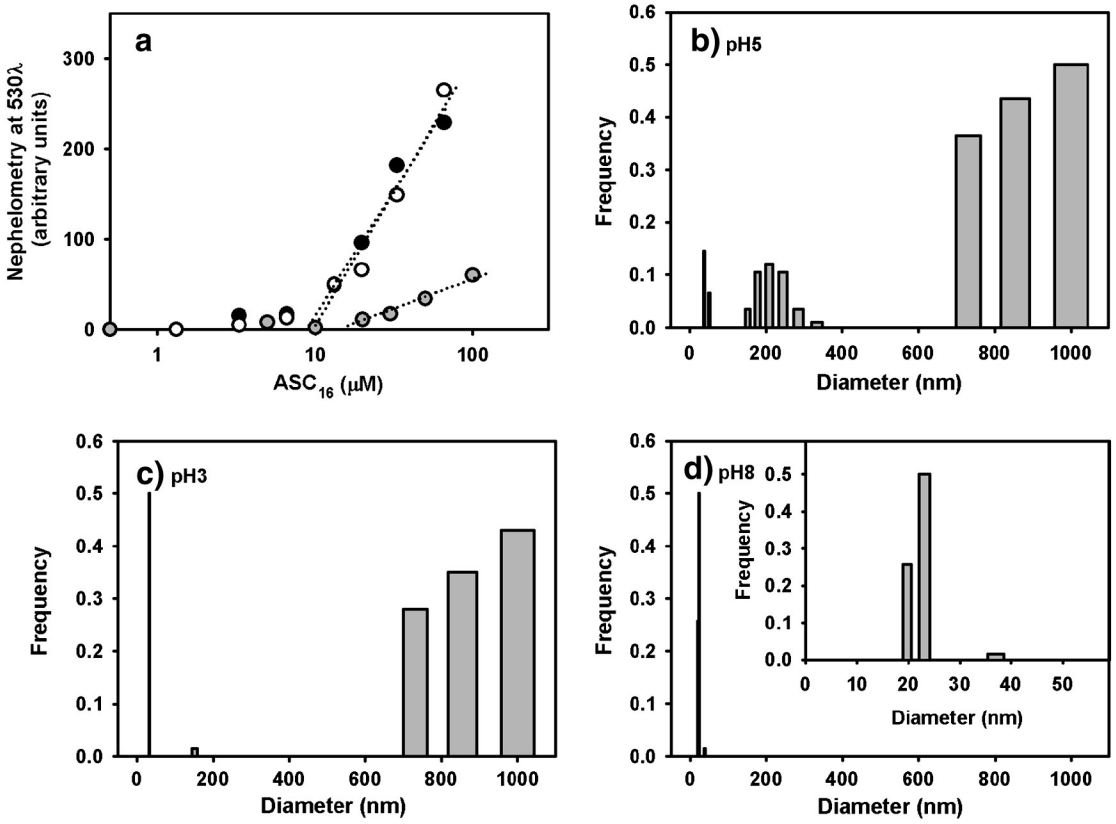

Fig. 7. Self-organized structures of ASC_{16} in the bulk saline solution for different pHs: (a) Nephelometry (b–d) and Dynamic light scattering studies of ASC_{16}-water suspension. In (a), black circles represent pH ~ 3, white circles pH ~ 5 and gray circles pH ~ 8 and dotted lines are for guide the eye. The results represent the average of two independent samples ± SEM. (b–d) show frequency of particle size for ASC_{16} solution (final concentration 18.5 μM) at pH ~ 3, pH ~ 5 and pH ~ 8, respectively. Inset in panel (d) shows an x-scale expansion. The frequency data in (c–d) represent the addition of two independent experiments.

3.5. The effect of rheological properties on ASC_{16} penetration of monolayers

The phase diagram reported from the Langmuir monolayers of pure ASC_{16} and saline pH 5 subphase [2] indicates that, at the π value reached in adsorption experiments (~35 mN/m), the film might be in an LC state. The LC phase of lipid membranes is characterized by a lower diffusion coefficient (compared to the LE state) [21], which may be an important constraint in ASC_{16} insertion to the already formed ASC_{16} monolayer, thus explaining the very slow rise in π in the adsorption experiments (see Fig. 2a). In contrast, the DMPC monolayers (in penetration experiments) provided a fluid LE character (evidenced by low Cs^{-1} values at low ASC_{16} proportions, Fig. 3c) to the binary DMPC + ASC_{16} resultant film. This effect may explain the faster penetration kinetics compared with the adsorption experiments.

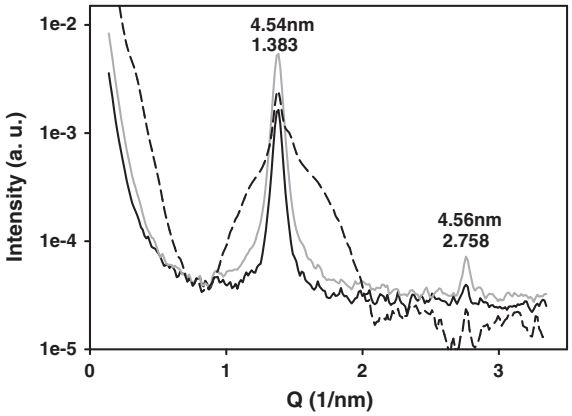

Fig. 8. SAXS of ASC_{16} at pH 3 (black full line), pH 5 (gray line) and pH 8 (black dashed line). Clear first order diffraction peaks are observed in all cases at 1.38 nm^{-1}. At pH 8, the peak is superimposed to a broad bump of diffuse scattering. The semi-logarithmic scale shows the second order peaks at ~2.76 nm^{-1}. The ASC_{16} final concentration was 5 mg/mL.

The above findings show the relevance of the rheological properties of the biological membrane on the ASC_{16} penetration kinetics. We further explored this aspect by introducing cholesterol (Chol) to the initial monolayer in the penetration experiments, as it is widely accepted that Chol alters the rheological properties of biological membranes and induces the formation of a liquid-ordered (LO) phase, both in the bilayer and monolayer systems [22,23]. This particular phase has the property of being extremely condensed (showing very high Cs^{-1} values) and at the same time maintaining a high fluidity of its components [24].

ASC_{16} penetration experiments to DMPC + Chol monolayers revealed that Chol favored the kinetic penetration process, with increasing proportions of Chol sharply lowering the penetration $t_{1/2}$ while slightly decreasing the equilibrium π (Fig. 9a and b). Interestingly, these effects were only observed at Chol proportions ≥25 mol%, where a LO-like character of the initial monolayer was evidenced by high Cs^{-1} values (see Fig. 9c). To investigate further this effect, we utilized Langmuir films of DMPC/Chol (60:40) with different proportions of ASC_{16}. The BAM visualization of these monolayers showed that Chol prevented the formation of the LC-ASC_{16}-enriched domains, whereas these domains were observed for the DMPC + ASC_{16} system at as low as 20 mol% ASC_{16} (Fig. 4b) and Fig. S2 shows that in the DMPC + Chol + ASC_{16} system they were observed at ≥65 mol% ASC_{16}. In this way Chol acts as a better molecular spacer between ASC_{16} molecules than DMPC, allowing the establishment of and homogeneously charged surface. Thus, Chol disturbed the DMPC + ASC_{16} LC phase in a similar way that it did in the gel

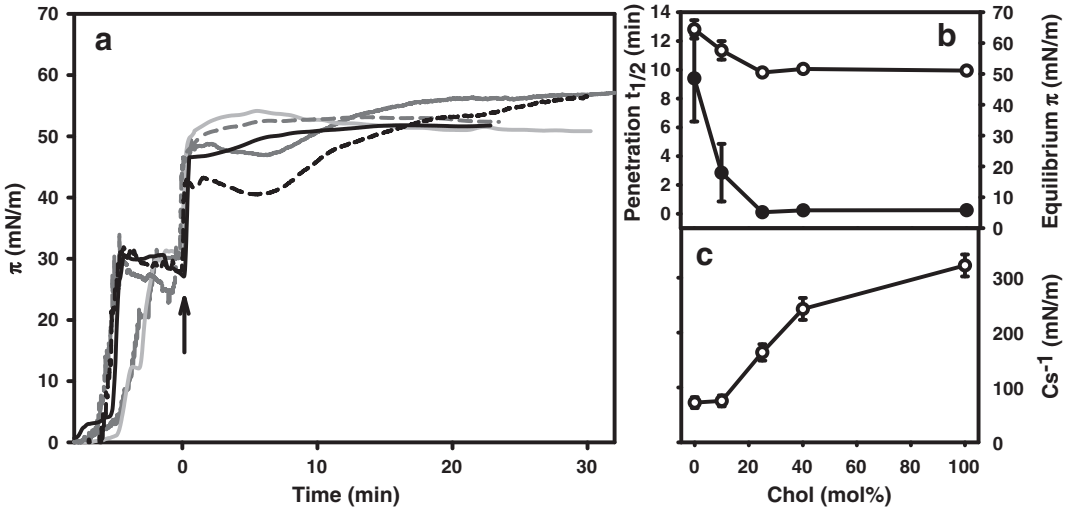

Fig. 9. Cholesterol (Chol) effect on the ASC_{16} penetration process. a) π-time curves corresponding to the penetration of ASC_{16} into DMPC and/or Chol monolayers at initially 30 mN/m, using 145 mM NaCl, pH ~ 5 as the subphase. Monolayer composition: pure Chol (black, full line), pure DMPC (black, dashed line), DMPC + Chol (90:10) (dark gray, full line), DMPC + Chol (75:25) (light gray, full line) and DMPC + Chol (60:40) (gray, dashed line). The arrow indicates the time of ASC_{16} injection into the subphase. The curves shown are chosen from a set of duplicates that differed by less than 3 mN/m. b) the equilibrium π (white circles) and the $t_{1/2}$ of the rise to the equilibrium (black circles) of the penetration experiments are plotted as a function of the monolayer initial lipid composition. c) Cs^{-1} of DMPC + Chol Langmuir films at 30 mN/m. The results are the average of two independent experiments ± SEM.

phase of PC bilayers [22]. It was probably due to its more fluid character that the Chol-enriched LO phase appeared more suitable to be penetrated by ASC_{16}.

4. Conclusions

In the present work, we showed that ASC_{16} is a potent amphiphile that can interact with lipid monolayers, with a cutoff point near the theoretical surface pressure limit (72 mN/m). The presence of a lipid film at the interface favored ASC_{16} insertion compared with a bare surface, which may have been due to the lipid film providing the resultant membranes with a fluid environment until being highly enriched in ASC_{16}. The adsorption and penetration time curves showed a biphasic behavior: the first rapid peak may have been a consequence of a fast adsorption of the charged ASC_{16} molecules to the interface and a posteriori lowering of surface pH, thus partially neutralizing the surface and compacting the film, with the second rise representing an equilibrium state between the subphase ASC_{16} and the binary phospholipid + ASC_{16} film. Based on the Langmuir DMPC + ASC_{16} monolayer data, the ASC_{16} partition coefficient to the DMPC film was estimated to be 1.5×10^5, which is larger than highly amphitropic proteins and drugs [13,18]. A large free energy of partition of $\Delta G_p = -6.7$ kcal·mol^{-1} was also calculated. It is worth pointing out that some of our conclusions are based on a cross-correlation between Gibbs and Langmuir monolayers. In agreement, previous studies by Vollhardt's group found an excellent correlation in the phase diagram of the Gibbs and Langmuir monolayers formed by amphiphilic amides, which was also confirmed by BAM visualization [25,26]. Unfortunately, however, our system did not allow us to verify a cross-correlation between the Langmuir and Gibbs monolayers by BAM since the subphase ASC_{16} aggregates in the adsorption and penetration experiments introduced a high background reflectivity that masked the visualization of the surface reflection.

The kinetic features of the ASC_{16} penetration depended on the electrostatic properties (i.e. the ionization state of the film), with the rheological properties of the host membrane also being determinant. The fluid membrane, as provided by Chol (LO phase), proved an excellent host membrane, probably due to the disruption of the LC ASC_{16}-enriched domains, being too rigid to allow further insertion of ASC_{16} molecules. The subphase conditions also affected the ASC_{16} aggregation in bulk, with big lamellar structures being favored at acidic pHs and smaller structures in alkaline conditions. These structures had a faster equilibrium with the surface film than the lamellar structures.

In summary, ASC_{16} interaction with model membranes revealed a highly complex regulation that involved the electrostatic and rheological properties of the host membrane and some polymorphism in its bulk aggregation, which resulted in a complex equilibrium between the surface and subphase forms of ASC_{16}. This work contributes to understanding the physical–chemical properties of this simple system (ASC_{16} + membrane), which may shed light on the pharmacological function of this drug.

Supplementary data to this article can be found online at http://dx.doi.org/10.1016/j.bbamem.2013.06.016.

Acknowledgements

This work was supported by: SECyT-UNC, FONCyT and CONICET. MM is an undergraduate student of Univesidad Nacional de Córdoba. LAB is a posdoctoral fellow and NW, RGO and MLF are Career Researchers of CONICET. RGO thanks the Brazilian Synchrotron Light Laboratory (CNPEM/MCT) for X-ray beamtime at SAXS2 beamline under project D11A–SAXS1–10716. We thank Dr. Paul Hobson, native speaker, for revision of the manuscript.

References

[1] L. Benedini, E.P. Schulz, P. Messina, S. Palma, D. Allemandi, P. Schulz, The ascorbyl palmitate–water system: phase diagram and state of water, Colloids Surf. A Physicochem. Eng. Asp. 375 (2011) 178–185.
[2] L. Benedini, M.L. Fanani, B. Maggio, N. Wilke, P. Messina, S. Palma, P. Schulz, Surface phase behavior and domain topography of ascorbyl palmitate monolayers, Langmuir 27 (2011) 10914–10919.
[3] G. Capuzzi, N.P. Lo, K. Kulkarni, J.E. Fernandez, Mixtures of stearoyl-6-O-ascorbic acid and α-tocopherol: a monolayer study at the gas/water interface, Langmuir 12 (1996) 3957–3963.
[4] J.F. Tocanne, J. Teissie, Ionization of phospholipids and phospholipid-supported interfacial lateral diffusion of protons in membrane model systems, Biochim. Biophys. Acta 1031 (1990) 111–142.
[5] J. Perez-Gil, C. Casals, D. Marsh, Interactions of hydrophobic lung surfactant proteins SP-B and SP-C with dipalmitoylphosphatidylcholine and dipalmitoylphosphatidylglycerol bilayers studied by electron spin resonance spectroscopy, Biochemistry 34 (1995) 3964–3971.
[6] F. Vega Mercado, B. Maggio, N. Wilke, Phase diagram of mixed monolayers of stearic acid and dimyristoylphosphatidylcholine. Effect of the acid ionization, Chem. Phys. Lipids 164 (2011) 386–392.

[7] G.L. Gaines, Insoluble Monolayers at Liquid–Gas Interfaces, Interscience Publishers, New York, 1966.
[8] U. Kohler, H.H. Mantsch, H.L. Casal, Infrared spectroscopic characterization of the interaction of ascorbyl palmitate with phospholipid bilayers, Can. J. Chem. 66 (1987) 983–988.
[9] I.D. Bianco, B. Maggio, Interactions of neutral and anionic glycosphingolipids with dilauroylphosphatidylcholine and dilauroylphosphatidic acid in mixed monolayers, Colloids Surf. 40 (1989) 249–260.
[10] N. Wilke, B. Maggio, The influence of domain crowding on the lateral diffusion of ceramide-enriched domains in a sphingomyelin monolayer, J. Phys. Chem. B 113 (2009) 12844–12851.
[11] M.L. Fanani, B. Maggio, Liquid–liquid domain miscibility driven by composition and domain thickness mismatch in ternary lipid monolayers, J. Phys. Chem. B 115 (2011) 41–49.
[12] R. Maget-Dana, The monolayer technique: a potent tool for studying the interfacial properties of antimicrobial and membrane-lytic peptides and their interactions with lipid membranes, Biochim. Biophys. Acta 1462 (1999) 109–140.
[13] P.L. de Matos Alves, S.V. Malheiros, A.C. Lino, P.E. de, M.A. Perillo, Hydroxyzine, promethazine and thioridazine interaction with phospholipid monomolecular layers at the air–water interface, Biophys. Chem. 119 (2006) 247–255.
[14] G. Capuzzi, N.P. Lo, K. Kulkarni, J.E. Fernandez, F.F. Vincieri, Interactions of 6-O-stearoylascorbic acid and vitamin K_1 in mixed Langmuir films at the gas/water interface, Langmuir 12 (1996) 5413–5418.
[15] G. Capuzzi, K. Kulkarni, J.E. Fernandez, F.F. Vincieri, N.P. Lo, Mixtures of ascorbyl-stearate and vitamin D3: a monolayer study at the gas/water interface, J. Colloid Interface Sci. 186 (1997) 271–279.
[16] A. Shaukat, J.M. Smaby, M. Momsen, H.L. Brockman, R.E. Brown, Acyl chain-length asymmetry alters the interfacial elastic interactions of phosphatidylcholines, Biophys. J. 74 (1998) 338–348.
[17] E.D. Goddard, O. Kao, C. Kung, Monolayer properties of fatty acids IV. Influence of cation at high pH, J. Colloid Sci. 24 (1967) 297–309.
[18] M.L. Fanani, B. Maggio, Kinetic steps for the hydrolysis of sphingomyelin by bacillus cereus sphingomyelinase in lipid monolayers, J. Lipid Res. 41 (2000) 1832–1840.
[19] S. Palma, R. Manzo, D. Allemandi, L. Fratoni, N.P. Lo, Coagels from ascorbic acid derivatives, Langmuir 18 (2002) 9219–9224.
[20] S. Palma, N.P. Lo, R. Manzo, D. Allemandi, Evaluation of the surfactant properties of ascorbyl palmitate sodium salt, Eur. J. Pharm. Sci. 16 (2002) 37–43.
[21] N. Wilke, F. Vega Mercado, B. Maggio, Rheological properties of a two phase lipid monolayer at the air/water interface: effect of the composition of the mixture, Langmuir 26 (2010) 11050–11059.
[22] J.H. Ipsen, G. Karlstrom, O.G. Mouritsen, H. Wennerstrom, M.J. Zuckermann, Phase equilibria in the phosphatidylcholine–cholesterol system, Biochim. Biophys. Acta 905 (1987) 162–172.
[23] H.M. McConnell, A. Radhakrishnan, Condensed complexes of cholesterol and phospholipids, Biochim. Biophys. Acta 1610 (2003) 159–173.
[24] G. Lindblom, G. Oradd, Lipid lateral diffusion and membrane heterogeneity, Biochim. Biophys. Acta 1788 (2009) 234–244.
[25] D. Vollhardt, V. Melzer, Phase transition in adsorption layers at the air–water interface: bridging to Langmuir monolayers, J. Phys. Chem. B 101 (1997) 3370–3375.
[26] D. Vollhardt, V.B. Fainerman, Characterisation of phase transition in adsorbed monolayers at the air/water interface, Adv. Colloid Interface Sci. 154 (2010) 1–19.